

Role of the C-Terminal 28 Residues of β 2-Microglobulin in Amyloid Fibril Formation[†]

Magdalena I. Ivanova,[‡] Mari Gingery,[‡] Lisa J. Whitson,[§] and David Eisenberg^{*,‡}

Howard Hughes Medical Institute and UCLA-DOE Institute of Genomics and Proteomics, BOX 951570, University of California—Los Angeles, Los Angeles, California 90095-1571

Received June 12, 2003

ABSTRACT: β 2microglobulin (β 2m) is the major protein component of the fibrillar amyloid deposits isolated from patients diagnosed with dialysis-related amyloidosis (DRA). While investigating the molecular mechanism of amyloid fibril formation by β 2m, we found that the β 2m C-terminal peptide of 28 residues ($c\beta$ 2m) itself forms amyloid fibrils. When viewed by electron microscopy, $c\beta$ 2m aggregates appear as elongated unbranched fibers, the morphology typical for amyloids. $c\beta$ 2m fibers stain with Congo red and show apple-green birefringence in polarized light, characteristic of amyloids. The observation that the β 2m C-terminal fragment readily forms amyloid fibrils implies that β 2m amyloid fibril formation proceeds via interactions of amyloid forming segments, which become exposed when the β 2m subunit is partially unfolded.

Amyloidosis is the process of protein aggregation associated with a variety of human degenerative diseases (1). These pathological amyloid aggregates consist of elongated fibers, resistant to disruption. The components of any given amyloid fibril are primarily of a single-type protein and may form from wild-type, mutant, or truncated proteins. Similar fibrils can be formed in vitro from oligopeptides and denatured proteins (2–4).

β 2-microglobulin (β 2m)¹ has been used as a model system to study the mechanism of amyloid fibril formation (5–8). Normally, β 2m is the light chain of the type I major histocompatibility complex responsible for the presentation of peptides to the immune system. In its native state, β 2m adopts a typical immunoglobulin fold consisting of seven β -strands organized into two β -sheets connected by a single disulfide bridge (9) (Figure 1a). In addition, β 2m has a pathological role. It was discovered to be the major component of the amyloid deposits taken from patients diagnosed with dialysis-related amyloidosis (DRA), a serious complication of long-term hemodialysis (10, 11).

Different segments of β 2m were isolated from ex vivo amyloid fibrils consisting of β 2m truncated at residues Ile7, Ser11, Gly18, Leu87 (12), and Ser20 (13). Also, two amyloid forming segments of β 2m were identified to be the Ser20 to Lys41 peptide (14) and the Asp59 to Ala79 peptide (15).

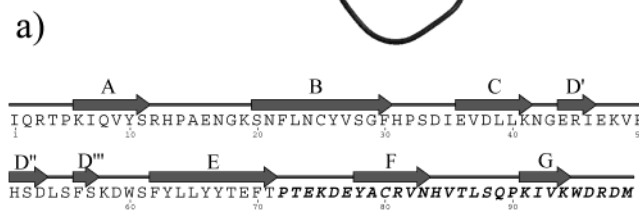


FIGURE 1: (a) Structure of β 2-microglobulin (β 2m). Ribbon diagram of human β 2m (PDB 3HLA) (9). The disulfide bond between Cys25 and Cys80 is drawn in ball-and-stick. The $c\beta$ 2m fragment encompasses the F and G β -strands (residues 72–99) and is shown in dark gray. (b) Sequence of β 2m. The amino acid sequence of the $c\beta$ 2m segment is in bold italics. The figure was drawn using MolScript (35) and SecSeq (36).

In this paper, we show that yet another β 2m segment ($c\beta$ 2m) encompassing the F and G β -strands (Figure 1; β 2m residues 72–99) aggregates to form fibrils, which also have properties common to amyloids.

EXPERIMENTAL PROCEDURES

β 2m and $c\beta$ 2m Overexpression and Purification. The gene encoding β 2m was subcloned from the pALUW31 vector into pET3a (Novagen). Four β 2m segments (β 2m residues

[†] This work was supported by NIH Grant GM31299 and NSF Grant MCB9904671.

^{*} Corresponding author. E-mail: david@mbi.ucla.edu.

[‡] Howard Hughes Medical Institute and UCLA-DOE Institute of Genomics and Proteomics.

[§] Present address: Department of Biochemistry, The University of Texas, Health Science Center at San Antonio, 7703 Floyd Curl Dr., San Antonio, TX 78229-3900.

¹ Abbreviations: DRA, dialysis-related amyloidosis; β 2m, β 2-microglobulin; $c\beta$ 2m, a β 2m segment spanning residues 72–99; GST, glutathione-S-transferase; CD, circular dichroism; EM, electron microscopy.

1–32, 33–71, 72–99, and 1–71) were cloned into the pGEX-4T vector (Amersham Pharmacia) to be expressed as glutathione-S-transferase (GST) fusion proteins. The plasmids were transformed into *Escherichia coli* BL21(DE3) (Novagen). The cells were grown at 37 °C in LB media with 100 μ g/mL ampicillin (Fischer) and induced at OD₆₀₀ 0.6 with 0.5 mM isopropyl β -D-thiogalactopyranoside (Fischer) for 3 h to produce protein.

β 2m was refolded using the protocol described in ref 16. After refolding, β 2m was purified on a size-exclusion silica G3000 column (Toso Haas). $C\beta$ 2m fused to GST was immobilized onto glutathione sepharose 4B (Amersham Pharmacia) and cleaved with thrombin (Amersham Pharmacia: 40 units per 1 mL bed volume of glutathione sepharose; 16 h at room temperature). The cleaved $c\beta$ 2m was further purified on a size-exclusion G3000 column (Toso Haas).

Electron Microscopy. Specimens were applied directly onto hydrophilic carbon-coated parlodion support films mounted on copper grids, allowed to adhere for 2 min, rinsed with distilled water, and stained with 1% uranyl acetate (Ted Pella, Inc.). Grids were examined in a Hitachi H-7000 electron microscope at an accelerating voltage of 75 kV.

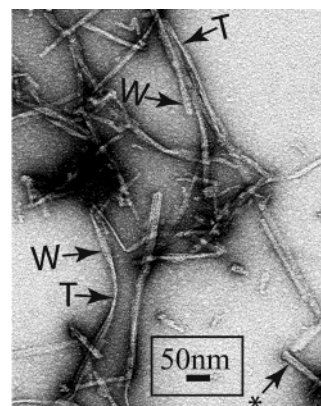
Circular Dichroism (CD). CD experiments were performed on a Jasco J-715 spectropolarimeter. Samples of 45 μ M $c\beta$ 2m were used to record spectra at room temperature in a 1 mm path-length cell with a 0.5 nm bandwidth, 0.5 nm resolution, 20 nm/min interval speed, and 8 s response time.

Congo Red Binding Assays. For birefringence analysis, the fibers were incubated with 120 μ M Congo red in 150 mM NaCl, 10 mM HEPES pH 8.0 for 30 min, sedimented by centrifugation at 20 000g for 1 min, washed three times with water, resuspended with 10 μ L of water, and dried on a glass slide to be examined by a light microscope. Spectroscopic assays were done as described in ref 17.

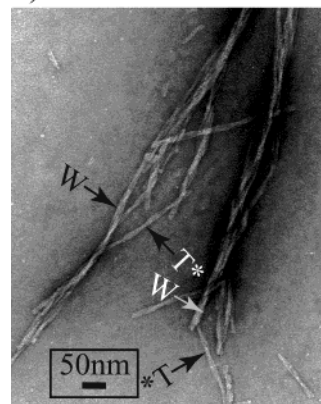
Polymerization and Dissociation Assays. Both assays were done at 37 °C. Fibrils were formed with shaking after dissolving 180 μ M lyophilized protein in 1.5 M NaCl, 25 mM phosphate buffer, pH 2.0. For fibril dissociation studies, preformed fibers (180 μ M total protein amount) were spun at 20 000g for 5 min and resuspended with 125 mM NaCl, 25 mM HEPES, pH 7.4.

RESULTS

Identifying $c\beta$ 2m as an Amyloid Forming Peptide. Initially, we partitioned the β 2m sequence into three segments (1–32; 33–71; 72–99) each about 30 residues in length. All segments when fused to GST were soluble, but we were able to cleave only the $c\beta$ 2m segment (β 2m residues 72–99). Then, we tested if the β 2m 1–71 segment could be purified, but it was expressed as inclusion bodies both when fused to GST and when not fused to GST. Consequently, we were not able to investigate if the 1–32, 33–71, and 1–71 segments could aggregate into amyloid fibrils. In contrast, $c\beta$ 2m fused to GST was soluble and easily cleaved. After screening various conditions, we found that $c\beta$ 2m forms fibrils at higher salt concentrations (1.0 M NaCl; 25 mM phosphate, pH 2.0) and a higher concentration (160 μ M) than β 2m. For comparison, β 2m forms fibrils at concentrations as low as 10 μ M and in solutions with as little as 50 mM NaCl (18).



a)



b)

FIGURE 2: Electron micrographs of $c\beta$ 2m and β 2m fibrils. (a) An electron micrograph of $c\beta$ 2m (160 μ M), incubated in 1.5 M NaCl and 25 mM phosphate buffer pH 2.0, reveals extended linear fibrils. On the basis of their diameters, these fibrils can be classified into thin (T) (5.0 ± 0.6 nm) and wide (W) (11.5 ± 1.2 nm). (b) Fibrils formed from β 2m (40 μ M) under the same conditions have diameters 7.2 ± 0.6 nm thin (T) and 13.1 ± 0.7 nm wide (W). Notice that $c\beta$ 2m fibrils are straighter than β 2m fibrils. However, both β 2m and $c\beta$ 2m fibrils are intertwined with alternating thinner and wider regions (arrows marked with *).

Characterization of $c\beta$ 2m Fibrils. $C\beta$ 2m fibrils are elongated and unbranched, morphology typical for amyloids. On the basis of their diameters, fibrils of $c\beta$ 2m can be divided into two groups: thin (T) (5.0 ± 0.6 nm) and wide (W) (11.5 ± 1.2 nm), Figure 2a. The thin fibrils may intertwine to form the thicker fibrils. β 2m fibrils can also be classified into two groups by their diameters: 7.2 ± 0.6 nm thin (T) and 13.1 ± 0.7 nm wide (W), Figure 2b. However, β 2m fibrils are less straight than $c\beta$ 2m fibrils.

$C\beta$ 2m aggregates bind Congo red (Figure 3a) and appear green when viewed between crossed polarizers (Figure 3b), both characteristics of amyloid fibrils (19). $C\beta$ 2m aggregates also show a red shift of visible light absorbance when stained with Congo red (Figure 3c), another amyloid characteristic (17). Notice that the maxima of the wild-type β 2m and $c\beta$ 2m absorption spectra are different: wild-type β 2m fibrils absorb maximally at 552 nm, whereas the maximum for $c\beta$ 2m is 542 nm. This maximum for $c\beta$ 2m is the same as that for $A\beta$ (1–40) amyloid fibrils—the major component of Alzheimer's plaques (20).

In neutral pH buffer, $c\beta$ 2m exists primarily as a coil (Figure 4), a conformation different from the mostly β -sheet β 2m. However, as typical for amyloids, an increase in β -sheet

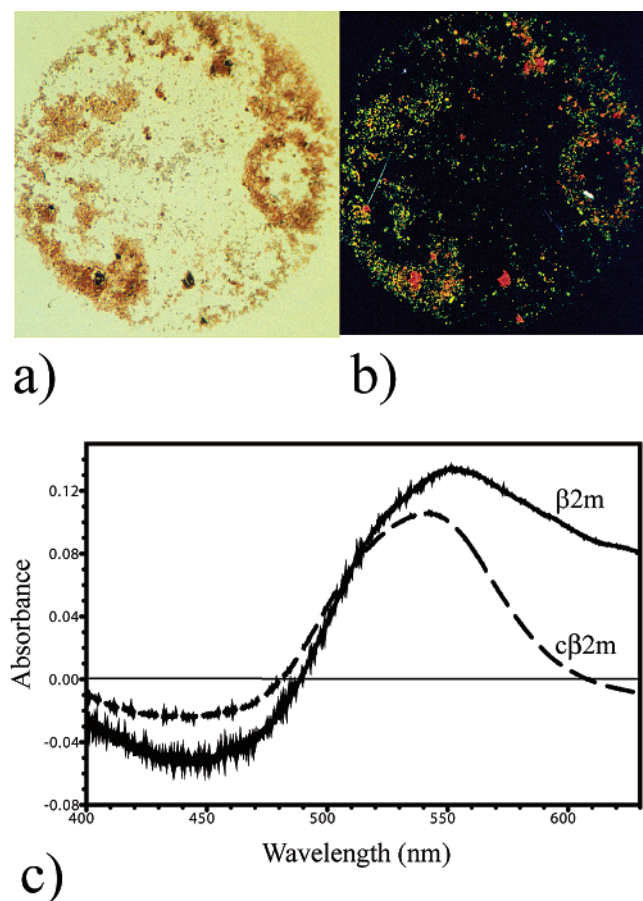


FIGURE 3: Congo red binding of $c\beta 2m$ and $\beta 2m$ aggregates. (a) $C\beta 2m$ fibrils stained with $120 \mu M$ Congo red solution are colored red when viewed under unpolarized light. (b) When viewed under cross-polarized light, the sample shown in panel a exhibits apple-green birefringence typical for amyloid fibrils. (c) Comparison between the difference spectra of the wild-type $\beta 2m$ (solid line) and $c\beta 2m$ (dashed line) fibers stained with Congo red. Both protein concentrations are the same ($160 \mu M$). The difference spectra shown here were calculated by subtracting the spectrum of Congo red in the absence of fibrils from the scatter corrected spectrum of the protein in the presence of Congo red. The difference spectrum was corrected for scatter by subtracting the spectrum of the fibrils without Congo red. Notice that the maxima of the difference spectrum of the $\beta 2m$ and $c\beta 2m$ fibers are at 552 and 542 nm, respectively.

content is observed in the CD spectrum taken immediately after the lyophilized $c\beta 2m$ is dissolved into buffer promoting fibril formation (2.5 M NaCl, 25 mM phosphate, pH 2.0; Figure 4). This increase in β -sheet content becomes even more pronounced after one week of incubation at 37 °C (Figure 4). Thus, the estimated β -sheet content of the week-old $c\beta 2m$ samples in high salt and low pH is about 37%, as compared to 20% when stored in high salt (2.5 M NaCl) and neutral pH buffer (Figure 4). Notice the presence of the characteristic β -sheet minimum at 218–220 nm in the CD spectrum of week-old $c\beta 2m$ in high salt and low pH buffer (Figure 4).

Monitoring $c\beta 2m$ Fibril Formation. Fibrils form upon transfer of $\beta 2m$ into a low pH buffer containing high salt (1.5 M NaCl, pH 2.0), and there is no lag phase in the aggregate formation (open rhombs, Figure 5). Similarly, McParland et al. (18) and Hong et al. (21) observed that $\beta 2m$ forms fibrils rapidly without a lag phase. In contrast, $c\beta 2m$ incubated at the same conditions does not appear to

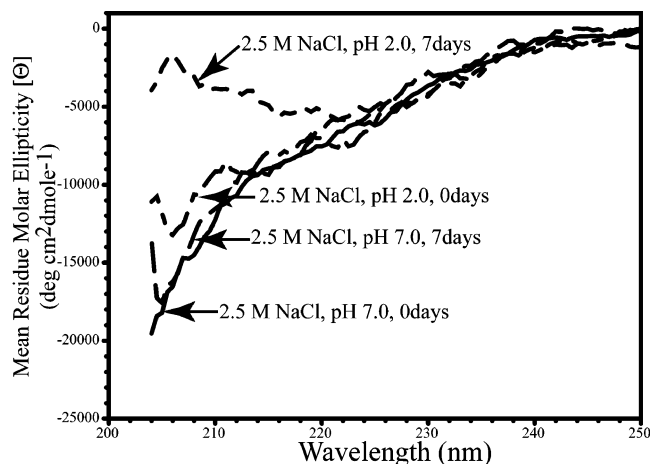


FIGURE 4: Far-ultraviolet CD spectra of $c\beta 2m$. Notice the change in circular dichroism in a high ionic strength (2.5 M NaCl) and low pH (pH 2.0) solution, which becomes more pronounced upon incubation of the protein for a week. Thus, the estimated β -sheet content of the week-old $c\beta 2m$ is about 37%, opposed to 20% for $c\beta 2m$ stored at neutral pH. There is a minimum at 218–220 nm, characteristic for the β -sheet, in the spectrum of a week-old $c\beta 2m$ sample incubated in a high salt and low pH solution.

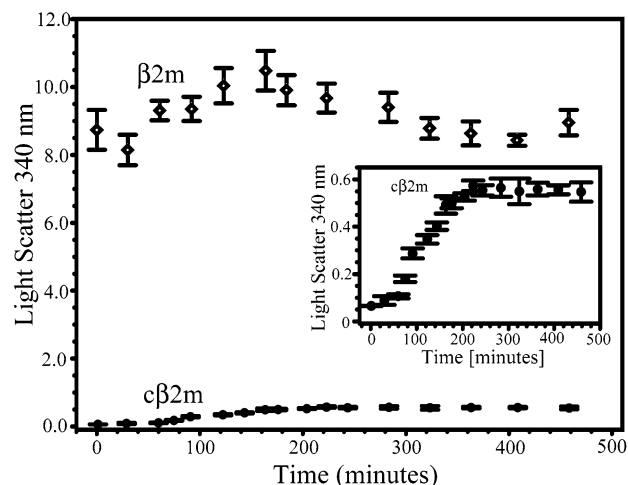


FIGURE 5: Comparison between fibril formation of $c\beta 2m$ (filled circles) and $\beta 2m$ (open rhombs), monitored by light scattering at 340 nm. The inset gives the time course of $c\beta 2m$ aggregation. $C\beta 2m$ fibers form with a lag time of 90 min, as opposed to wild-type $\beta 2m$, which aggregates immediately upon transfer into 1.5 M NaCl and pH 2.0 buffer.

aggregate until more than 90 min after the initiation of the reaction (inset and filled circles, Figure 5). In addition, $\beta 2m$ and $c\beta 2m$ differ in the aggregated state. The scattering intensity of the $\beta 2m$ aggregates is about 15 times higher than the scattering intensity of the $c\beta 2m$ fibrils. Thus, $c\beta 2m$ fibrils form less efficiently than $\beta 2m$ fibrils.

Stability of $\beta 2m$ and $c\beta 2m$ Fibrils in Physiological Buffers. After transfer into pH 7.4 buffer, most of the $c\beta 2m$ fibrils/aggregates dissociate in the first 30 min, as judged by light scattering measurements (Figure 6a). For comparison, $\beta 2m$ fibrils/aggregates dissociate in about 100 min—about three times more slowly than $c\beta 2m$ fibrils (Figure 6b). Similarly, Kozhukh et al. (14) reported that $\beta 2m$ fibrils dissociate more slowly than fibers formed of another amyloid-like $\beta 2m$ segment (residues Ser20 to Lys41).

Electron micrographs of $c\beta 2m$ and $\beta 2m$ samples incubated for 3 days at pH 7.4 are shown in Figure 7. A sheetlike

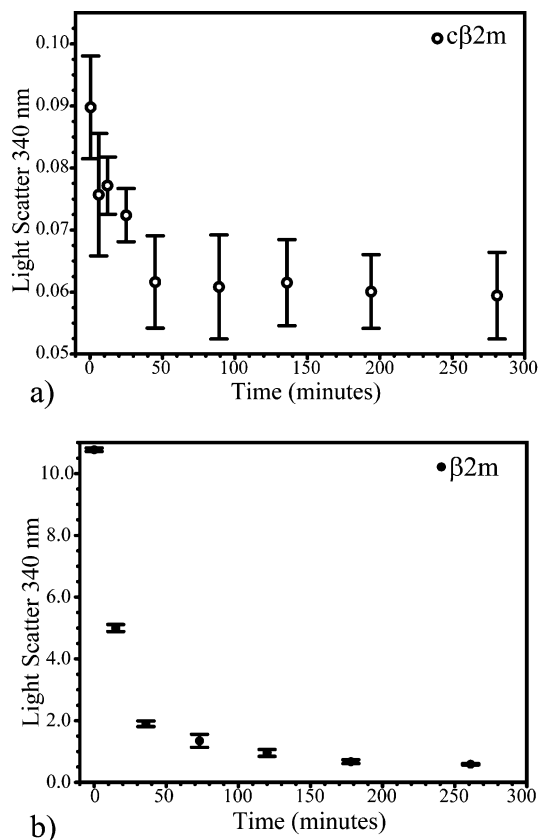


FIGURE 6: Dissociation of $c\beta 2m$ and $\beta 2m$ fibrils formed in vitro. Fibrils of $c\beta 2m$ and $\beta 2m$ were incubated at 37 °C in HEPES buffer (125 mM NaCl, pH 7.4). The time course of turbidity shows that some $c\beta 2m$ aggregates (a) dissociate in the first 30 min and some $\beta 2m$ aggregates (b) dissociate in 100 min.

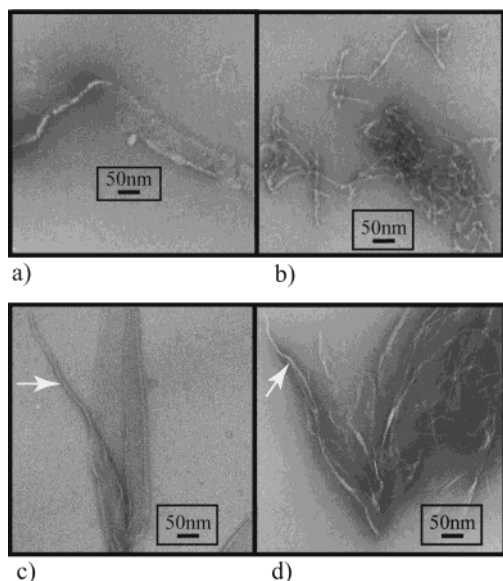


FIGURE 7: Both $c\beta 2m$ and $\beta 2m$ fibrils dissociate when stored at pH 7.4. There is only sheetlike material (a) and bundles of thin fibrils (b) when $c\beta 2m$ fibrils are incubated at pH 7.4 for 3 days. Similarly, a sheet like-material (c) and bundles of fibrils (d) are observed in $\beta 2m$ samples incubated at pH 7.4 for 3 days. The few amyloid-like fibrils observed in the $\beta 2m$ sample are shown with arrows in panels c and d.

material was found in both samples (Figure 7a,c). The $\beta 2m$ specimen contained few amyloid-like fibers (shown with white arrows—Figure 7c,d) and bundles of thin fibrils

(Figure 7d). In contrast, only short fibers and bundles of thin fibrils were observed in the $c\beta 2m$ sample (Figure 7b).

DISCUSSION

Figures 2 and 3 show that $c\beta 2m$ aggregates form long fibrils and that these fibers bind Congo red, both properties commonly observed in amyloids. The importance of $c\beta 2m$ in the context of $\beta 2m$ fibril formation is supported by the finding that an antibody raised against $\beta 2m$ residues 92–99 inhibits fibril formation in vitro (22). In contrast, antibodies against 20–41 and 63–75 do not inhibit fibril formation (22), which suggests that $c\beta 2m$ ($\beta 2m$ residues 72–99) is the determinant of the propensity of $\beta 2m$ to aggregate into amyloid fibrils.

Our observation that the F and G β -strands ($c\beta 2m$; Figure 1) are sufficient for amyloid fibril formation implies their importance in $\beta 2m$ fibril formation. Jones et al. (15) showed that neither the F β -strand nor the G β -strand forms fibrils. Therefore, only when F and G β -strands are fused together can they form fibrils. In conditions favorable for fibril formation, the G β -strand, but not the F β -strand, is solvent exposed (7, 8). Thus, the fiber formation may be due to exposure of residues in the F and G β -strand connecting segment (His84 to Pro90).

Besides $c\beta 2m$, segments $\beta 2m$ 20–41 (14), 59–71 (15), and 59–79 (15) were found by others to form fibrils. To compare these four amyloid forming segments of $\beta 2m$, we examined properties that have been found by others to correlate with the ability of the peptide to form amyloid fibrils, such as hydrophobicity (23), β -sheet propensity (24), the arrangement of the hydrophobic and hydrophilic residues (25), the net charge (26), and the number of aromatic residues (27). All these segments and the full-length $\beta 2m$ have similar propensities to form a β -sheet (28, 29). Depending on the hydrophobicity scale, we found that each segment has at least a four residue-long segment with alternating hydrophobic/hydrophilic residues (30, 31). The 21–40 segment (14) has the longest segment (six residues—Kyte and Doolittle scale (30) and seven residues—Eisenberg et al. scale (31)) of alternating hydrophobic/hydrophilic residues. Other than alternating hydrophobic/hydrophilic residues, there seems to be little in common among all four segments.

$C\beta 2m$ fibrils form less efficiently than $\beta 2m$ fibrils (Figure 5). One explanation of the slower fibril growth is that $\beta 2m$ nucleates faster than $c\beta 2m$, which might be due to other amyloid determining factors, such as a missing amyloid forming segment from the $c\beta 2m$ peptide (14, 15). An alternative explanation is that prior to or during nucleation, $c\beta 2m$ undergoes a slow transition from coil to β -sheet (Figure 4). In contrast, $\beta 2m$ has high β -sheet content in its native state (Figure 1), and there is no evidence of conformational changes in the protein subunits during fibril assembly. A similar conformational transition was proposed to be one of the contributing factors to the lag phase of the Alzheimer's A β fibril formation (32).

Fibrils of the $c\beta 2m$ protein dissociate faster than $\beta 2m$ fibrils (Figure 6). This may be explained by the lack of stabilizing interactions from the rest of the protein. A number of different segments of $\beta 2m$ have been proposed to be important in the fibril assembly including the B and C β -strands (14), the edge of strand D (33), and the E β -strand

(15) (Figure 1). These segments of $\beta 2m$, in addition to elements of $c\beta 2m$, may participate in $\beta 2m$ fibril formation.

The knowledge of the $\beta 2m$ regions that are involved in fibril formation may aid in the design of compounds that could then be inhibitors of amyloid formation. A similar strategy was successfully used to delay the onset of Alzheimer's disease in mice (34), where antibodies raised against a fragment of A β (residues Phe4 to Tyr10) have strong antifibrillogenic properties.

ACKNOWLEDGMENT

We thank Drs. Gary Kleiger and Ralf Landgraf for discussions and Drs. Tara Chapman and P. Bjorkman (Caltech, Pasadena, CA) for $\beta 2m$ plasmid DNA.

REFERENCES

1. Westermark, P., Benson, M. D., Buxbaum, J. N., Cohen, A. S., Frangione, B., Ikeda, S., Masters, C. L., Merlini, G., Saraiva, M. J., and Sipe, J. D. (2002) *Amyloid* 9, 197–200.
2. Reches, M., Porat, Y., and Gazit, E. (2002) *J. Biol. Chem.* 277, 35475–80.
3. Balbirnie, M., Grothe, R., and Eisenberg, D. S. (2001) *Proc. Natl. Acad. Sci. U.S.A.* 98, 2375–80.
4. Burke, M. J., and Rougvie, M. A. (1972) *Biochemistry* 11, 2435–9.
5. Chiti, F., Mangione, P., Andreola, A., Giorgetti, S., Stefani, M., Dobson, C. M., Bellotti, V., and Taddei, N. (2001) *J. Mol. Biol.* 307, 379–91.
6. Esposito, G., Michelutti, R., Verdone, G., Viglino, P., Hernandez, H., Robinson, C. V., Amoresano, A., Dal Piaz, F., Monti, M., Pucci, P., Mangione, P., Stoppini, M., Merlini, G., Ferri, G., and Bellotti, V. (2000) *Protein Sci.* 9, 831–45.
7. Hoshino, M., Katou, H., Hagihara, Y., Hasegawa, K., Naiki, H., and Goto, Y. (2002) *Nat. Struct. Biol.* 9, 332–6.
8. McParland, V. J., Kalverda, A. P., Homans, S. W., and Radford, S. E. (2002) *Nat. Struct. Biol.* 9, 326–31.
9. Bjorkman, P. J., Saper, M. A., Samraoui, B., Bennett, W. S., Strominger, J. L., and Wiley, D. C. (1987) *Nature* 329, 506–12.
10. Gejyo, F., Yamada, T., Odani, S., Nakagawa, Y., Arakawa, M., Kunitomo, T., Kataoka, H., Suzuki, M., Hirasawa, Y., Shirahama, T. et al. (1985) *Biochem. Biophys. Res. Commun.* 129, 701–6.
11. Casey, T. T., Stone, W. J., DiRaimondo, C. R., Brantley, B. D., DiRaimondo, C. V., Gorevic, P. D., and Page, D. L. (1986) *Hum. Pathol.* 17, 731–8.
12. Bellotti, V., Stoppini, M., Mangione, P., Sunde, M., Robinson, C., Asti, L., Brancaccio, D., and Ferri, G. (1998) *Eur. J. Biochem.* 258, 61–7.
13. Linke, R. P., Bommer, J., Ritz, E., Waldherr, R., and Eulitz, M. (1986) *Biochem. Biophys. Res. Commun.* 136, 665–71.
14. Kozhukh, G. V., Hagihara, Y., Kawakami, T., Hasegawa, K., Naiki, H., and Goto, Y. (2002) *J. Biol. Chem.* 277, 1310–5.
15. Jones, S., Manning, J., Kad, N. M., and Radford, S. E. (2003) *J. Mol. Biol.* 325, 249–57.
16. Garboczi, D. N., Hung, D. T., and Wiley, D. C. (1992) *Proc. Natl. Acad. Sci. U.S.A.* 89, 3429–33.
17. Klunk, W. E., Pettegrew, J. W., and Abraham, D. J. (1989) *J. Histochem. Cytochem.* 37, 1273–81.
18. McParland, V. J., Kad, N. M., Kalverda, A. P., Brown, A., Kirwin-Jones, P., Hunter, M. G., Sunde, M., and Radford, S. E. (2000) *Biochemistry* 39, 8735–46.
19. DeLellis, R. A., Glenner, G. G., and Ram, J. S. (1968) *J. Histochem. Cytochem.* 16, 663–5.
20. Klunk, W. E., Jacob, R. F., and Mason, R. P. (1999) *Methods Enzymol.* 309, 285–305.
21. Hong, D. P., Gozu, M., Hasegawa, K., Naiki, H., and Goto, Y. (2002) *J. Biol. Chem.* 277, 21554–60.
22. Stoppini, M., Bellotti, V., Mangione, P., Merlini, G., and Ferri, G. (1997) *Eur. J. Biochem.* 249, 21–6.
23. Wurth, C., Guimard, N. K., and Hecht, M. H. (2002) *J. Mol. Biol.* 319, 1279–90.
24. Villegas, V., Zurdo, J., Filimonov, V. V., Aviles, F. X., Dobson, C. M., and Serrano, L. (2000) *Protein Sci.* 9, 1700–8.
25. Wang, W., and Hecht, M. H. (2002) *Proc. Natl. Acad. Sci. U.S.A.* 99, 2760–5.
26. Chiti, F., Calamai, M., Taddei, N., Stefani, M., Ramponi, G., and Dobson, C. M. (2002) *Proc. Natl. Acad. Sci. U.S.A.* 99 Suppl. 4, 16419–26.
27. Gazit, E. (2002) *FASEB J.* 16, 77–83.
28. Chou, P. Y., and Fasman, G. D. (1978) *Annu. Rev. Biochem.* 47, 251–76.
29. Deleage, G., and Roux, B. (1987) *Protein Eng.* 1, 289–94.
30. Kyte, J., and Doolittle, R. F. (1982) *J. Mol. Biol.* 157, 105–32.
31. Eisenberg, D., Wilcox, W., and McLachlan, A. D. (1986) *J. Cell. Biochem.* 31, 11–7.
32. Hasegawa, K., Yamaguchi, I., Omata, S., Gejyo, F., and Naiki, H. (1999) *Biochemistry* 38, 15514–21.
33. Trinh, C. H., Smith, D. P., Kalverda, A. P., Phillips, S. E., and Radford, S. E. (2002) *Proc. Natl. Acad. Sci. U.S.A.* 99, 9771–6.
34. McLaurin, J., Cecal, R., Kierstead, M. E., Tian, X., Phinney, A. L., Manea, M., French, J. E., Lambermon, M. H., Darabie, A. A., Brown, M. E., Janus, C., Chishti, M. A., Horne, P., Westaway, D., Fraser, P. E., Mount, H. T., Przybylski, M., and St. George-Hyslop, P. (2002) *Nat. Med.* 8, 1263–9.
35. Kraulis, P. J. (1991) *J. Appl. Cryst.* 24, 946–50.
36. Brodersen, D. E. <http://xray.imsb.au.dic/~deb/secseq>.

BI0301486